Journal of Materials Chemistry B

Accepted Manuscript

ROYAL SOCIETY OF CHEMISTRY

www.rsc.org/materialsB

Journal of Materials Chemistry B

COMMUNICATION

Antineoplastic Busulfan encapsulated in Metal Organic Framework nanocarrier: first *in vivo* results

Received 00th January 20xx,
Accepted 00th January 20xx

DOI: 10.1039/x0xx00000x

www.rsc.org/

M.T. Simon-Yarza,[a] T. Baati,[a] A. Paci,[b] L.L. Lesueur,[b] A. Seck,[b] M. Chiper,[c] R. Gref,[c] C. Serre,[a] P. Couvreur,[c] P. Horcajada[b]†

Nanoparticles of the mesoporous iron(III) trimesate MIL-100 nanocarrier encapsulating high amounts of the challenging antineoplastic busulfan were administered to rats and compared with the commercial Busilvex®. Large differences in serum concentration of both busulfan and trimesate revealed the great impact of drug encapsulation both on the drug and nanoparticle pharmacokinetics during the first 24 h.

Busulfan (Bu), an antineoplastic alkylsulfonate agent, designated as butane-1,4-diyl dimethane sulfonate, was firstly used in 1959 and received the Food and Drug Administration (FDA) approval in 1999 to treat chronic myeloid leukemia (CML)[1]. Nowadays it represents the cornerstone of many commonly used regimes in hematopoietic stem cell transplantation[2]. The mechanism of action corresponds to that of an alkylating agent, preventing from DNA replication due to the crosslinks taking place between guanine-adenine and guanine-guanine[3]. Two different formulations of Bu have been developed and registered: 2mg oral tablets Myleran® (Aspen) used mainly in CML and intravenous solution Busilvex® (Pierre Fabre Ltd.) at 6 $mg.mL^{-1}$. Busilvex® is the corner stone of conditioning regimen prior to hematopoietic stem cell transplantation (HSCT) and bone marrow transplantation, in leukemia, lymphoma, myeloproliferative disorders and especially in pediatrics in immunodeficiency and inborn errors[4,5]. However, several limitations can be pointed out: i) both intravenous and oral administration lead to large inter-patient variability, two times greater after oral administration that also drives important differences in the bioavailability[6-8], ii) high systemic levels of the drug are associated to hepatic veno-occlusive disease, originally considered as a consequence of the Bu crystallization[9] but nowadays contemplated as a result of the interaction between Bu and Melphalan[4], iii) the limited aqueous solubility of Bu obliges the use of organic solvents, such as N,N-dimethylacetamide in Busilvex®, with the associated toxicity risks[10], moreover, iv) in contact with aqueous solutions, Bu is rapidly hydrolyzed (into tetrahydrofuran and methanesulphonic acid) and inactivated[11,12]. These shortfalls justify the efforts invested to develop new Bu delivery formulations[13]. Among them, incorporating this agent into nanocarriers offers several advantages, including i) protection of the drug from degradation before reaching the target, ii) prolonged release of the drug, accompanied by a iii) reduction of the administered dose with subsequent adverse effects, and iv) reduction of the inter- and intra-patient heterogeneous bioavailability. Liposomes and polymers (such as poly(isobutylcyanoacrylate)[14] and polyester-PEG diblock copolymers[13]) have been evaluated to perform Bu encapsulation, leading to very poor payloads (< 1 wt%), exceptionally reaching 6 wt% in specific polymeric systems[14]. Some of us succeeded to incorporate the highest Bu loadings achieved to date (up to 26±3 wt%) into original nanocarriers based on porous Metal-Organic Framework nanoparticles (nanoMOFs)[15]. In particular, the large porosity (BET surface ~ 1500 $m^2.g^{-1}$, pore volume ~ 1.2 $cm^3.g^{-1}$) associated with a suitable amphiphilic internal environment (metal cation and organic linker) allowed the iron(III) trimesate (BTC) MIL-100 (MIL stands for Material Institute Lavoisier) nanoparticles (NPs)[16], to incorporate exceptional Bu loadings (up to 36±4 wt%) without altering NP size (always kept within 140±25) and to release the drug in a prolonged way [17], preventing Bu from its crystallization and degradation, as proven by the release of its intact active form[18]. In addition, these NPs have shown absence of any *in vivo* toxicity, even upon the intravenous administration of very high doses (220 $mg.kg^{-1}$)[19]. They also display interesting imaging properties[15], making them promising nanocarriers for Bu administration.

These very interesting results have encouraged us to perform

[a] Institut Lavoisier, UMR8180 CNRS, Université de Versailles St-Quentin en Yvelines, Versailles Cedex, France;
[b] Service de Pharmacologie, UMR CNRS 8203, Gustave-Roussy Cancer Campus, Villejuif Cedex, France
[c] Institut Galien, UMR8612 CNRS, Université Paris-Sud, Châtenay-Malabry, France
† Corresponding author. E-mail address: patricia.horcajada@uvsq.fr. Electronic Supplementary Information (ESI) available: [details of any supplementary information available should be included here]. See DOI: 10.1039/x0xx00000x

the first pharmacokinetics (PK) preclinical studies of the Bu-loaded MIL-100 NPs, evaluating both the drug and BTC serum levels, as well as their accumulation in organs 24 h after intravenous administration. Although the external surface modification of nanoMOFs has been recently proposed as an interesting route to modify the *in vivo* fate of NPs, the novelty of this approach together with the need to compare these strategies with the uncoated NPs, make necessary to evaluate the PK of the simpler bared Bu-loaded MIL-100 NPs. Therefore, MIL100 without any modification was here used. The administered doses were figured out considering the standard regimes of Bu (3.2 $mg.kg^{-1}.day^{-1}$). Therefore, considering NPs with 32 wt% Bu content, animals received 13.0 $mg.kg^{-1}$ of the Bu-loaded MIL-100 NPs, 3.2 $mg.kg^{-1}$ of Busilvex® and 9.8 $mg.kg^{-1}$ of non-loaded NPs (named MIL100-Bu, Bu and MIL100 groups, respectively). It should be mentioned that the total Bu administered dose is the same in both animal groups.

Remarkably, Bu PK profiles showed that the Bu detected after MIL100-Bu administration was much lower than after Busilvex® dosage with a mean Bu area under the serum concentration versus time curve (AUC) of 2.6 *vs.* 25 µg/ml·min respectively (Fig. 1). It should be mentioned that the total Bu administered dose is the same in both animal groups. After intravenous administration of Busilvex®, all Bu is available in the blood from the first moment. However, in the MIL100-Bu group, the drug is supposed to be released throughout time from the porous NPs, until their capture by tissues, their metabolization and excretion from the organism, which may explain the lower serum concentration. This means that one could rationally expect that Bu will be protected within the pores of MIL100 from degradation in the medium, leading to, *a priori,* controlled release associated with higher efficacy. Nevertheless, further *in vivo* studies are required to verify the prolonged effect of the MIL100-Bu treatment as a consequence of this prolonged release of the drug.

When comparing BTC PK of MIL100-Bu and MIL100, important differences in maximum serum concentration were observed (Fig.1). After administration of the empty MIL100 NPs and during the first 30 min, serum levels of BTC remained close to 4 % of the administered dose. This concentration felt down during the following hours, up to only 0.5 % of the administered dose after 8 h. In contrast, BTC serum concentration in rats treated with the MIL100-Bu NPs after 30 min reached only 0.5 % of the administered dose and was undetectable after 2 h. This could be explained by a difference in surface charge between the empty and Bu-loaded NPs. Indeed, native NPs exhibit a negatively charged surface (-23±5 mV quantified by Laser Doppler Micro-electrophoresis), whereas encapsulation of Bu leads to a positive ζ-potential value (+13±5 mV). The presence of the amphiphilic Bu adsorbed on the outer surface of the NPs could be at the origin of this switch. Native MIL100 NPs have a characteristic hydrophilic and acidic surface, consequence of the partially coordinated Lewis acidic iron(III) sites, as well as free BTC carboxylic groups (pKa ~ 3.5-4.5) which governs the surface charge of the NPs. One can assume that Bu exposed on the external surface of the NP interact with the free iron sites which would lead to both a hydrophobic character as well as a different surface charge behavior. Indeed, it has been demonstrated that hydrophobic positively charged surfaces suffer from opsonization and subsequent clearance by the immune system in a greater rate than more hydrophilic surfaces[20,21]. One therefore expects here that the adhesion of proteins covering the particles in a corona-like way could affect i) the recognition by the macrophages, leading to a faster elimination from the blood stream, ii) the Bu release kinetics via the alteration of the drug diffusion through the protein layer, and iii) the modification of the chemical and physical stability of the NPs, either protecting or boosting the degradation of the NPs. To better understand these points, it must be reminded that drug release from porous MOFs is determined by different mechanisms, namely a) MOF progressive degradation due to interaction with physiological media, b) drug-matrix interaction and/or c) diffusion of the drug through the pores. Observed results are in accordance with a slow-down diffusion of the drug through the protein coating. Observations show how serum levels of both Bu and BTC are reduced in the MIL100-Bu group compared to the control groups. These positively-charged more hydrophobic particles would be opsonized and recognized by the macrophages in a faster manner than in the case of treatment with MIL100. This explains why clearance of the NPs is higher after treatment with MIL100-Bu (Cl = 23.32 $mL.min^{-1}$, $t_{1/2}$ = 1.6 h) than with negatively charged MIL100 (Cl = 0.75 $mL.min^{-1}$, $t_{1/2}$ = 5.4 h). Note however that NPs could be partially chemically degraded in the blood, leading to a BTC release, affecting the quantified serum levels.

Fig. 1. Left: Trimesic acid average serum levels expressed on a logarithmic scale as % of total BTC administered after administration of non-loaded (MIL100) and loaded (MIL100-Bu) nanoparticles (* indicates that concentration was found below the quantification limit). Right: Bu average serum levels plotted on a logarithmic scale after intravenous administration of Busilvex® and loaded nanoparticles

Fig. 2. BTC accumulated in the different organs 24 h after MIL100 (red) and MIL100-Bu (yellow) administration. BTC in urine after 8 and 24 h is also represented. Values express the % of total administered BTC. (n.d.: non-detected values).

On the other hand, preliminary 24 h-biodistribution (BD) study of MIL100 NPs has been performed by assessing the BTC content in different organs (liver, spleen, kidneys and lungs). An important accumulation of the NPs in the reticulo-endothelial system (liver and spleen) is observed. If one compares these data with previously reported BD results obtained after administration of twenty-times higher doses of MIL100 NPs, we observe how BTC concentration is

approximately 3 times higher after high dose NP injection (in liver: 13±3 *vs*. 35±8 %, and in spleen: 1.0±0.3 *vs*. 3.0±0.9 % when 9.8 or 220 mg.kg^{-1} were administered, respectively)[19] evidencing a significant effect of the administered dose. Despite the BD pattern is almost the same for both doses, majority of the NPs are accumulated in the liver and, in a more discrete amount, in spleen. This is partially due to the larger weight of the liver but also to a greater accumulation, as confirmed by the higher hepatic concentration (18±5 µg.g^{-1} in liver *vs*. 11±2 µg.g^{-1} in spleen). It is noteworthy that no significant differences were found on the accumulation of the NPs loaded or not with Bu (Fig. 2). Apparently, this would not be in accordance with our previous hypothesis, *i.e*. a greater clearance of the MIL100-Bu in comparison with MIL100 as a consequence of the different surface charge. After NP opsonization, macrophages and other phagocytic cells recognize and phagocyte them, travelling through the bloodstream to accumulate principally in liver and spleen, in which higher accumulation of the Bu-loaded NPs should be observed[22]. Nevertheless, one must be cautious and bear in mind that these data correspond to 24 h after the administration; early times must be investigated to reach a more accurate conclusion. In fact, it has been reported that the majority of the NPs are cleared from the blood in less than 5 min[22].

Finally, excretion of the NPs was also assessed by BTC quantification in urine and feces. Results of urinary excretion show greater BTC levels in urine after MIL100-Bu administration both at 8 and 24 h than after MIL100 NPs injection, suggesting that empty NPs are excreted in a faster way than the loaded ones. This could be due to the more observed rapid clearance from the blood stream of MIL100-Bu leading to faster elimination. Misfortunately, these data cannot be compared to fecal excretion since it was not possible to collect a significant amount of feces in all groups, due to the very short times of the study.

Conclusions

Previously reported results confirmed that MIL100 NPs are able to delay the delivery of Bu keeping its cytotoxic activity intact. Thus, the encapsulation of Bu into NPs is a promising strategy to improve the efficacy of this first-line alkylating agent of conditioning regimen prior to HSCT or BMT used in severe and rare diseases. On the one hand, this work demonstrates how Bu encapsulation into MIL100 NPs drastically modifies the PK of the drug and of the BTC during the first 8 h. On the other hand, no differences in the accumulation in organs after 24 h were observed, although this study must be completed with earlier BD times. Particles were rapidly eliminated from the body, as observed in urine samples, being the elimination faster for the empty NPs. Differences observed between MIL100 and MIL100-Bu were probably due to the inversion of the surface charge from negative to a positive after incorporation of the drug.

Recently, some of us reported a promising strategy to delay protein adhesion or opsonization of MIL100-Bu, increasing thus their circulation half-life (frequently known as "stealth" NPs) and leading to different BD and/or passive cancer targeting, by decorating the outer surface of the MIL100 NPs with biopolymers such as heparin[23]. This method could be applied in a near future to MIL100-Bu to reduce the clearance of these NPs and increase the efficacy of the treatment.

Acknowledgement

This work was partially supported by the CNRS, Université Paris Sud, Université de Versailles Saint-Quentin and funded through the Nanogalenic project from the Pole de Competitivité MEDICEN, ERC-2007-209241-BioMOFs and the French Research Agency (ANR) through a VirMIL MatePro ANR-project and a "Investissements d'Avenir" program (Labex NanoSaclay, ref: ANR-10-LABX-0035).

References

1 Z. Hassan, M. Hassan and E. Hellström-Lindberg, *Leukemia*, 2001, **15**, 1240–1247.

2 A. Paci, G. Veal, C. Bardin, D. Levêque, N. Widmer, J. Beijnen, A. Astier and E. Chatelut, *Eur. J. Cancer*, 2014, **50**, 2010–9.

3 T. Iwamoto, Y. Hiraku, S. Oikawa, H. Mizutani, M. Kojima and S. Kawanishi, *Cancer Sci.*, 2004, **95**, 454–458.

4 A. Galaup and A. Paci, *Expert Opin. Drug Metab. Toxicol.*, 2013, **9**, 333–47.

5 S. O. Ciurea and B. S. Andersson, *Biol. Blood Marrow Transplant.*, 2009, **15**, 523–36.

6 G. J. Veal, L. Nguyen, A. Paci, M. Riggi, M. Amiel, D. Valteau-Couanet, P. Brock, R. Ladenstein and G. Vassal, *Eur. J. Cancer*, 2012, **48**, 3063–72.

7 S. Choe, G. Kim, H.-S. Lim, S.-H. Cho, J.-L. Ghim, J. A. Jung, U.-J. Kim, G. Noh, K.-S. Bae and D. Lee, *Korean J. Physiol. Pharmacol.*, 2012, **16**, 273–80.

8 M. Hassan, G. Oberg, A. N. Bekassy, J. Aschan, H. Ehrsson, P. Ljungman, G. Lönnerholm, B. Smedmyr, A. Taube and I. Wallin, *Cancer Chemother. Pharmacol.*, 1991, **28**, 130–4.

9 M. F. Ozkaynak, K. Weinberg, D. Kohn, L. Sender, R. Parkman and C. Lenarsky, *Bone Marrow Transplant.*, 1991, **7**, 467–74.

10 H. P. Bhagwatwar, S. Phadungpojna, D. S. Chow and B. S. Andersson, *Cancer Chemother. Pharmacol.*, 1996, **37**, 401–8.

11 M. Hassan and H. Ehrsson, *J. Pharm. Biomed. Anal.*, 1986, **4**, 95–101.

12 M. Houot, V. Poinsignon, L. Mercier, C. Valade, R. Desmaris, F. Lemare and A. Paci, *Drugs R. D.*, 2013, **13**, 87–94.

13 J. Bouligand, P. Couvreur, A. M. Layre, A. Deroussent, A. Paci, E. Delain, G. Vassal and R. Gref, *J. Microencapsul.*, 2007, **24**, 715–30.

14 A. Layre, P. Couvreur, H. Chacun, J. Richard, C. Passirani, D. Requier, J. P. Benoit and R. Gref, *J. Control. Release*, 2006, **111**, 271–80.

15 P. Horcajada, T. Chalati, C. Serre, B. Gillet, C. Sebrie, T. Baati, J. F. Eubank, D. Heurtaux, P. Clayette, C. Kreuz, J.-S. Chang, Y. K. Hwang, V. Marsaud, P.-N. Bories, L. Cynober, S. Gil, G. Férey, P. Couvreur and R. Gref, *Nat. Mater.*, 2010, **9**, 172–8.

16 P. Horcajada, S. Surblé, C. Serre, D.-Y. Hong, Y.-K. Seo, J.-S. Chang, J.-M. Grenèche, I. Margiolaki and G. Férey, *Chem. Commun. (Camb).*, 2007, 2820–2.

17 M.G. Chiper, P. Horcajada, G. Maurin, L.L. Lesueur , A. Seck , A. Paci, P. Couvreur, C. Serre, R. Gref, *Unpublished*, 2015.

18 T. Chalati, P. Horcajada, P. Couvreur, C. Serre, M. Ben Yahia, G. Maurin and R. Gref, *Nanomedicine (Lond).*, 2011, **6**, 1683–95.

19 T. Baati, L. Njim, F. Neffati, A. Kerkeni, M. Bouttemi, R. Gref, M. F. Najjar, A. Zakhama, P. Couvreur, C. Serre and P. Horcajada, *Chem. Sci.*, 2013, **4**, 1597–1607.

20 G. Sahay, D. Y. Alakhova and A. V. Kabanov, *J. Control. Release*, 2010, **145**, 182–195.

21 K. Kettler, K. Veltman, D. van de Meent, A. van Wezel and a. J. Hendriks, *Environ. Toxicol. Chem.*, 2014, **33**, 481–492.

22 M. C. Garnett and P. Kallinteri, *Occup. Med. (Lond).*, 2006, **56**, 307–11.

23 E. Bellido, T. Hidalgo, M. V. Lozano, M. Guillevic, R. Simón-Vázquez, M. J. Santander-Ortega, Á. González-Fernández, C. Serre, M. J. Alonso and P. Horcajada, *Adv. Healthc. Mater.*, 2015.

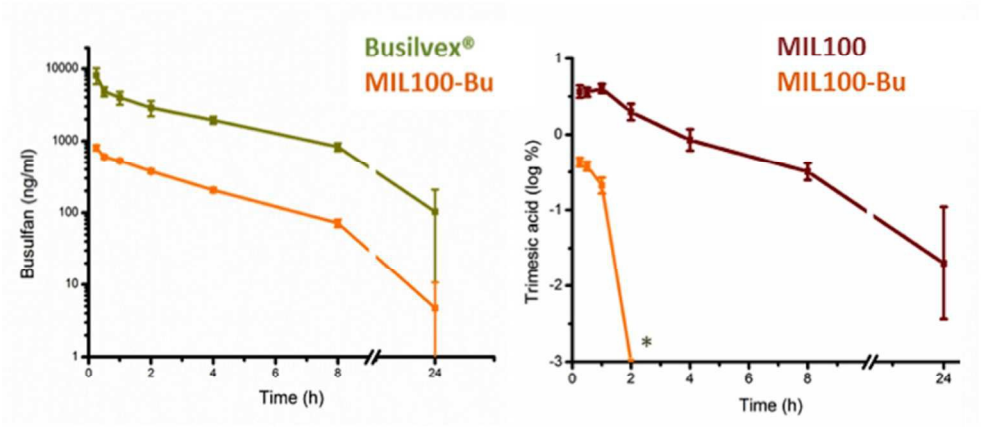

90x67mm (300 x 300 DPI)

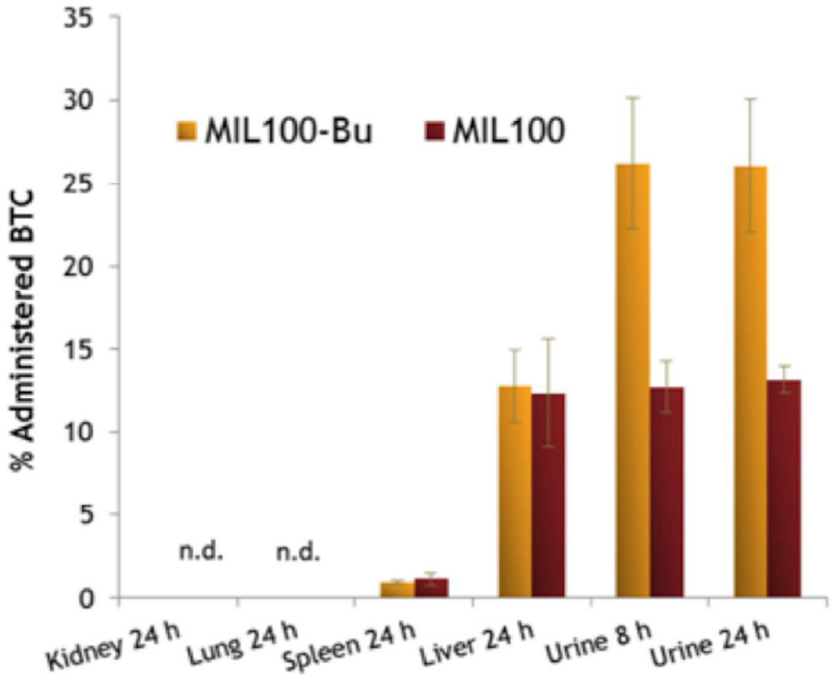

90x67mm (300 x 300 DPI)

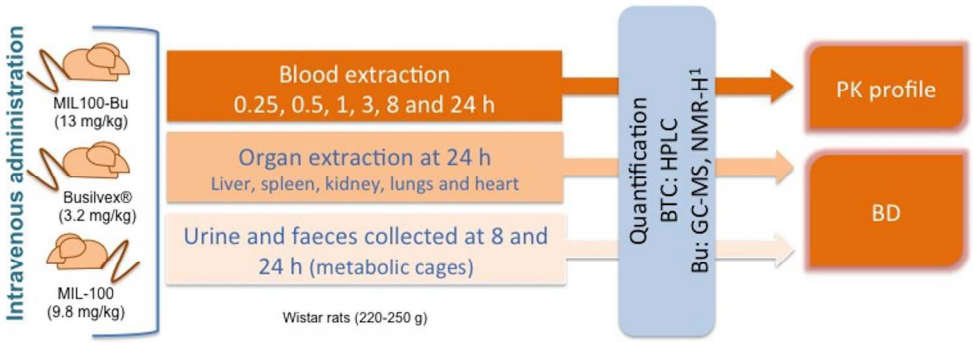

967x333mm (72 x 72 DPI)